

# MAGNETO-OPTICAL INVESTIGATION OF THE VORTEX ORDER-DISORDER PHASE TRANSITION IN BSCCO

B. Kalisky<sup>1</sup>, A. Shaulov<sup>1</sup>, T. Tamegai<sup>2</sup> and Y. Yeshurun<sup>1</sup>

*1. Institute of Superconductivity, Department of Physics, Bar-Ilan University, Ramat-Gan 52900, Israel*

*2. Department of Applied Physics, The University of Tokyo, Hongo, Bunkyo-ku, Tokyo 113-8656, Japan*

Abstract:

Time resolved magneto-optical technique is employed to trace the time evolution of the second magnetization peak (SMP) in  $\text{Bi}_2\text{Sr}_2\text{CaCu}_2\text{O}_{8+\delta}$  at different temperatures. The results show that the external field and induction marking the onset of the SMP exhibit entirely different temperature and time dependence. The differences are attributed to variations of the local magnetization with time and temperature. The implications of these findings on measurements of the thermodynamic order-disorder vortex phase transition line are discussed.

Key words: Vortex phase transitions; transient vortex state; second magnetization peak

The vortex order-disorder phase transition has been investigated extensively during recent years [1-9]. This transition is driven by both, thermally and disorder induced fluctuations of the vortices. Thermal fluctuations, dominating at high temperatures, cause a ‘melting’ transition [3], while disorder-induced fluctuations, dominating at low temperatures, cause a ‘solid – solid’ transition [10-17]. The magnetic signature of the transition varies considerably along the unified [8, 9, 18, 19] order-disorder transition line; While the melting transition is manifested by a sharp jump in the reversible magnetization, the solid-solid transition is marked by the onset of a second magnetization peak (SMP) in the irreversible magnetization.

Strong dynamic effects associated with the SMP, impede exact determination of the solid – solid transition induction in conventional magnetization measurements [6, 15, 19-30]. These dynamic effects have been attributed to transient disordered vortex states (TDVS), which are inevitably created by injection of vortices through inhomogeneous surface barriers while the external magnetic field increases [31, 32] or by "supercooling" of the disordered vortex phase while the field decreases [33, 34].

In a previous paper [24, 35] we described a time resolved magneto-optical technique, which allows the generation of instantaneous local magnetization curves at different locations on the sample surface. The time evolution of these curves demonstrates the annealing process of the TDVS and the emergence of a time dependent SMP. These measurements clearly show that the induction,  $B_{on}$ , at the onset of the SMP signifies a non-equilibrium transition to a transient disordered vortex state, and that  $B_{on}$  shifts with time upward, approaching the thermodynamic order-disorder transition induction,  $B_{od}$ . Time dependent measurements of the SMP reported in the literature show, however, inconsistent results: Hall probe measurements in Y-Ba-Cu-O [6, 30] and SQUID measurements in La-Sr-Cu-O [27-29] show that the onset of the SMP shifts to lower fields with time, while for Bi-Sr-Ca-Cu-O, some measurements show shift of the SMP onset to higher fields [19, 21-23, 26], and others to lower fields [19, 26]. Ignorance of the dynamic behavior of the SMP has led to qualitatively different reports on the behavior of the order-disorder transition line [5-7, 9, 18, 19, 22, 28, 36-40]. In this work we employ our time resolved magneto-optical technique to resolve this apparent inconsistency, and discuss the implications of our findings on the actual shape of the order-disorder phase transition line.

Measurements were performed on a  $1.55 \times 1.25 \times 0.05 \text{ mm}^3$   $\text{Bi}_2\text{Sr}_2\text{CaCu}_2\text{O}_{8+\delta}$  (BSCCO) single crystal ( $T_c \sim 92 \text{ K}$ ), grown by the traveling solvent floating zone method [41]. The external magnetic field,  $H$ , was raised abruptly to a target value between 140 and 840 G with rise-time  $< 50 \text{ ms}$ . Immediately after reaching the target field, magneto optical (MO) snapshots of the induction distribution across the sample surface were recorded at time intervals of 40 ms for 4 seconds, and 200 ms for additional 26 seconds, using iron-garnet MO indicator and a high speed CCD camera. This procedure was conducted at several temperatures between 20 and 30 K. Measurements were repeated in a commercial SQUID (Quantum Design - MPMS-5s), with time resolution of 1 min, between 16-30 K.

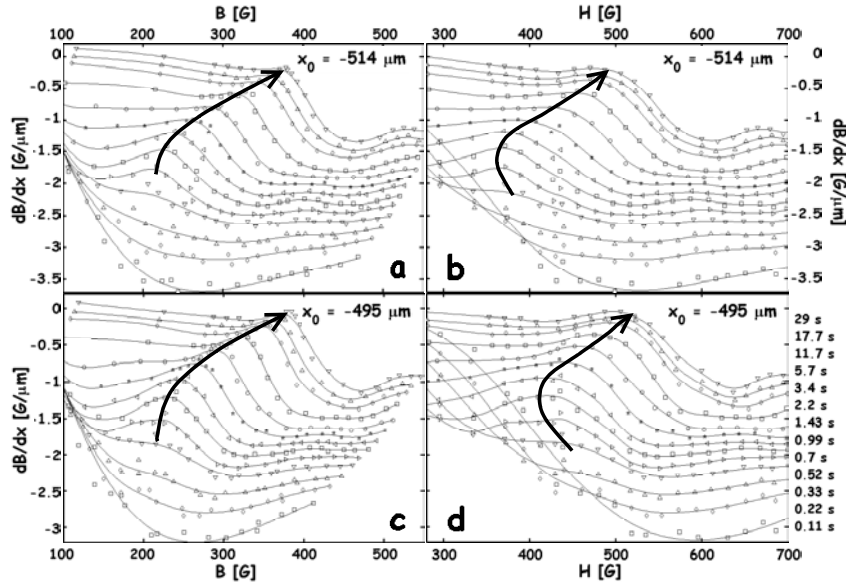


Figure 1. Time evolution of local  $j \sim dB/dx$  vs. B (a, c) or H (b, d), at the indicated times, measured at 21 K, for  $x_0 = -514 \mu\text{m}$  (a, b) and  $x_0 = -495 \mu\text{m}$  (c, d) measured from sample center.

From the MO images we extract the time evolution of the induction profiles across the sample width. On the basis of these data, we generate instantaneous local magnetization curves in the following way. For a certain location,  $x_0$ , along the sample width we extract the local  $j \sim dB/dx$  vs. B or H, at different times for all measured external fields. Connecting all data points corresponding to the same time generates an instantaneous magnetization curve. Typical results, measured at 21 K, are presented in Figure 1 for  $x_0 = -514 \mu\text{m}$  and  $x_0 = -495 \mu\text{m}$ , measured from the sample center. In the figure, data points corresponding to different times are marked by a different symbol and the solid lines connect all points measured at the same indicated time. Each curve represents an instantaneous local magnetization curve, and the set of curves demonstrates the time evolution of the second magnetization peak (SMP). Note that at short times ( $t < 0.5$  s), no SMP is observed, since initially the injected TDVS occupy the whole sample in the entire field range. A striking difference is observed between the time evolutions of  $j$  vs B and  $j$  vs H curves. While in  $j$  vs B curves (figure 1a and 1c) the onset induction,  $B_{\text{on}}$ , of the SMP shifts monotonically to higher inductions, in  $j$  vs H curves (figure 1b and 1d), the onset  $H_{\text{on}}$  initially shifts to lower fields and then at some point reverses its direction and shifts to higher fields. This effect is more pronounced at locations closer to sample center, as observed by comparing figures 1b and 1d. Furthermore, while

qualitatively similar time dependence of  $B_{on}$  is observed, independent of temperature, the behavior of  $H_{on}$  is strongly temperature dependent as demonstrated by the global measurements presented in Figure 2. For temperatures higher than 22 K,  $H_{on}$  always increases with time, as illustrated in Figure 2a for  $T = 23$  K. For temperatures lower than 20 K,  $H_{on}$  always decreases with time as illustrated in Figure 2b for  $T = 19.5$  K. In the intermediate temperature range, between 20 and 22 K,  $H_{on}$  exhibits a non-monotonic behavior; it initially decreases with time, and after reaching a minimum value, it increases with time, as illustrated in Figure 2c for  $T = 21$  K.

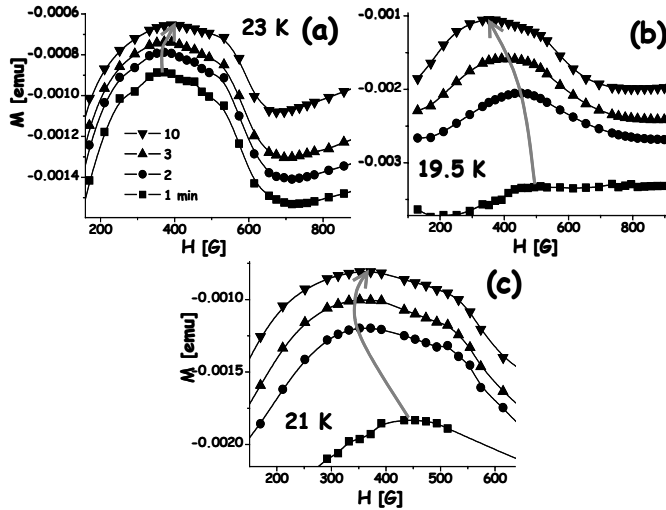


Figure 2. Time evolution of magnetization curves during 10 minutes after field application, demonstrating the various time dependencies of  $H_{on}$ . For  $T = 23$  K,  $H_{on}$  shifts to the right (a), for  $T = 19.5$  K,  $H_{on}$  shifts to the left (b), and for  $T = 21$  K,  $H_{on}$  exhibits a non monotonic behavior: initially it shifts to the left and then to the right (c).

Plotting these results in the  $H - T$  plane, one obtains a time dependent non-equilibrium ‘transition line’ as shown in Figure 3. The theoretically unexpected sharp decrease of the line at low temperature has been discussed by de Andrade *et al.* [42], and attributed to surface barriers [43-47]. It is interesting to note that  $H_{on}$  decreases with time in the temperature range corresponding to the theoretically unexpected falling branch of the line, and increases with time in the temperature range corresponding to the rising branch of the line. Completely different picture is obtained in the  $B - T$  diagram (see Figure 4). Here, the falling branch of the line is absent, and a monotonic increase of  $B_{on}$  is observed throughout the entire temperature range. The increase of the line with temperature is

restrained with time, as the rate of change of  $B_{on}$  with time decreases with increasing temperature [24]. The thermodynamic phase transition line is obtained in the limit of  $t \rightarrow \infty$ , and the above results show a trend of approaching a constant value at low temperatures as expected theoretically [48-50]. Clearly,  $B - T$  rather than  $H - T$  diagrams are relevant to the vortex phase diagram, and the above results demonstrate how far these two lines can be.

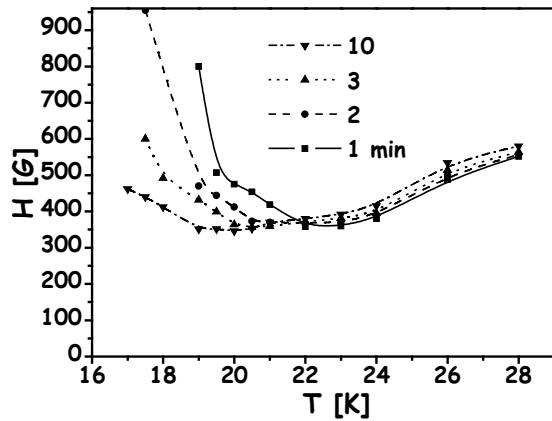


Figure 3. Time evolution of the measured transition line in the  $H$ - $T$  plane. Lines are extracted from the time dependence of  $H_{on}$  presented in figure 2 for different temperatures.

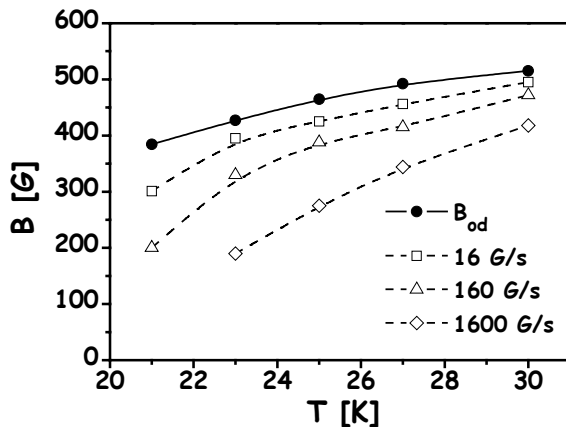


Figure 4. ‘Transition lines’ in the  $B - T$  plane, measured at the indicated sweep rates of the external magnetic field. Higher sweep rate corresponds to shorter experimental time window. Solid line presents the estimated thermodynamic transition line [24, 25, 51].

A simple explanation to the differences between H – T and B – T diagrams is based on the relationship:  $H_{on} = B_{on} + 4\pi|M|$ , where M is the local magnetization. Thus,

$$dH_{on}/dt = dB_{on}/dt + 4\pi d|M|/dt.$$

This equation implies that the rate of change of  $H_{on}$  is determined by sum of two competing terms: the rate of change of  $B_{on}$ , which is always *positive* and the rate of change of  $|M|$ , which is always *negative*. These two terms represent two different processes: the former is associated with the annealing of TDVS, while the latter is associated with thermally activated vortex creep over surface barriers [43-47]. At low temperatures  $d|M|/dt$  dominates, and thus  $dH_{on}/dt < 0$ , i.e.,  $H_{on}$  decreases with time. At high temperatures,  $dB_{on}/dt$  dominates, thus  $dH_{on}/dt > 0$ , i.e.,  $H_{on}$  increases with time. Since both  $d|M|/dt$  and  $dB_{on}/dt$  depend on time, a non-monotonic behavior of  $H_{on}$  may be obtained at intermediate temperatures. The sign of  $dH_{on}/dt$  is changed from negative to positive at a point where the value of  $d|M|/dt$  drops below the value of  $dB_{on}/dt$ . A detailed quantitative analysis will be given elsewhere.

In conclusion,  $H_{on}$  and  $B_{on}$  exhibit entirely different dependence on temperature and time. The differences can be attributed to variations of the local magnetization with time and temperature. For the determination of the order-disorder transition line,  $B_{on}$  is clearly more relevant. While global magnetic measurements yield  $H_{on}(T)$  which is affected by both, TDVS and surface barriers, local magnetic measurements, employing MO techniques, provide  $B_{on}(T)$  which is affected only by TDVS. The behavior of  $B_{on}(T)$  at long times approaches the behavior of the thermodynamic order-disorder phase transition line.

Acknowledgments: We thank D. Sylman for his help in measurements. We acknowledge support from the German-Israel Foundation (GIF). Y.Y. acknowledges support from the ISF Center of Excellence Program, and by the Heinrich Hertz Minerva Center for High Temperature Superconductivity.

1. R. Cubitt, E.M. Forgan, G. Yang, S.L. Lee, D.M. Paul, H.A. Mook, M. Yethiraj, P.H. Kes, T.W. Li, A.A. Menovsky, Z. Tarnawski, and K. Mortensen, Nature **365**, 407 (1993).

2. S.L. Lee, P. Zimmermann, H. Keller, M. Warden, R. Schauwecker, D. Zech, R. Cubitt, E.M. Forgan, P.H. Kes, T.W. Li, A.A. Menovsky, and Z. Tarnawski, *Phys. Rev. Lett.* **71**, 3862 (1993).
3. E. Zeldov, D. Majer, M. Konczykowski, V.B. Geshkenbein, V.M. Vinokur, and H. Shtrikman, *Nature* **375**, 373 (1995).
4. B. Khaykovich, E. Zeldov, D. Majer, T.W. Li, P.H. Kes, and M. Konczykowski, *Phys. Rev. Lett.* **76**, 2555 (1996).
5. K. Deligiannis, P.A.J. deGroot, M. Oussena, S. Pinfold, R. Langan, R. Gagnon, and L. Taillefer, *Phys. Rev. Lett.* **79**, 2121 (1997).
6. D. Giller, A. Shaulov, Y. Yeshurun, and J. Giapintzakis, *Phys. Rev. B* **60**, 106 (1999).
7. M. Baziljevich, D. Giller, M. McElfresh, Y. Abulafia, Y. Radzyner, J. Schneck, T.H. Johansen, and Y. Yeshurun, *Phys. Rev. B* **62**, 4058 (2000).
8. Y. Radzyner, A. Shaulov, and Y. Yeshurun, *Phys. Rev. B* **65**, 100513/1 (2002).
9. N. Avraham, B. Khaykovich, Y. Myasoedov, M. Rappaport, H. Shtrikman, D.E. Feldman, T. Tamegai, P.H. Kes, M. Li, M. Konczykowski, K. van der Beek, and E. Zeldov, *Nature* **411**, 451 (2001).
10. M. Daeumling, J.M. Seuntjens, and D.C. Larbalestier, *Nature* **346**, 332 (1990).
11. S.B. Roy and P. Chaddah, *Phys. C* **279**, 70 (1997).
12. L. Krusin-Elbaum, L. Civale, V.M. Vinokur, and F. Holtzberg, *Phys. Rev. Lett.* **69**, 2280 (1992).
13. Y.V. Bugoslavsky, A.L. Ivanov, A.A. Minakov, and S.I. Vasyurin, *Phys. C* **233**, 67 (1994).
14. V.N. Kopylov, A.E. Koshelev, I.F. Schegolev, and T.G. Togonidze, *Phys. C* **170**, 291 (1990).
15. V. Hardy, A. Wahl, A. Ruyter, A. Maignan, C. Martin, L. Coudrier, J. Provost, and C. Simon, *Phys. C* **232**, 347 (1994).
16. L. Klein, E.R. Yacoby, Y. Yeshurun, A. Erb, G. Muller-Vogt, V. Breit, and H. Wuehl, *Phys. Rev. B* **49**, 4403 (1994).
17. S. Bhattacharya and M.J. Higgins, *Phys. Rev. Lett.* **70**, 2617 (1993).
18. B. Khaykovich, M. Konczykowski, E. Zeldov, R.A. Doyle, D. Majer, P.H. Kes, and T.W. Li, *Phys. Rev. B* **56**, R517 (1997).
19. Y. Yamaguchi, G. Rajaram, N. Shirakawa, A. Mumtaz, H. Obara, T. Nakagawa, and H. Bando, *Phys. Rev. B* **63**, 014504/1 (2000).
20. Y. Yeshurun, N. Bontemps, L. Burlachkov, and A. Kapitulnik, *Phys. Rev. B* **49**, 1548 (1994).
21. H. Kupfer, A. Will, R. Meier-Hirmer, T. Wolf, and A.A. Zhukov, *Phys. Rev. B* **63**, 214521 (2001).
22. H. Kupfer, T. Wolf, R. Meier-Hirmer, and A.A. Zhukov, *Phys. C* **332**, 80 (2000).
23. M. Konczykowski, C.J. van der Beek, S. Colson, M.V. Indenbom, P.H. Kes, Y. Paltiel, and E. Zeldov, *Phys. C* **341**, 1317 (2000).
24. B. Kalisky, A. Shaulov, and Y. Yeshurun, *Phys. Rev. B* **68**, 012502 (2003).
25. B. Kalisky, D. Giller, A. Shaulov, and Y. Yeshurun, *Phys. Rev. B* **67**, R140508 (2003).
26. S. Anders, R. Parthasarathy, H.M. Jaeger, P. Guptasarma, D.G. Hinks, and R. van Veen, *Phys. Rev. B* **58**, 6639 (1998).
27. Y. Radzyner, A. Shaulov, Y. Yeshurun, I. Felner, K. Kishio, and J. Shimoyama, *Phys. Rev. B* **65**, 214525 (2002).
28. Y. Radzyner, A. Shaulov, Y. Yeshurun, I. Felner, K. Kishio, and J. Shimoyama, *Phys. Rev. B* **65**, 100503 (2002).
29. Y. Kodama, K. Oka, Y. Yamaguchi, Y. Nishihara, and K. Kajimura, *Phys. Rev. B* **56**, 6265 (1997).
30. Y. Abulafia, A. Shaulov, Y. Wolfus, R. Prozorov, L. Burlachkov, Y. Yeshurun, D. Majer, E. Zeldov, H. Wuhl, V.B. Geshkenbein, and V.M. Vinokur, *Phys. Rev. Lett.* **77**, 1596 (1996).

31. C.J. van der Beek, S. Colson, M.V. Indenbom, and M. Konczykowski, *Phys. Rev. Lett.* **84**, 4196 (2000).
32. D. Giller, A. Shaulov, T. Tamegai, and Y. Yeshurun, *Phys. Rev. Lett.* **84**, 3698 (2000).
33. Y. Paltiel, E. Zeldov, Y.N. Myasoedov, H. Shtrikman, S. Bhattacharya, M.J. Higgins, Z.L. Xiao, E.Y. Andrei, P.L. Gammel, and D.J. Bishop, *Nature* **403**, 398 (2000).
34. Y. Paltiel, E. Zeldov, Y. Myasoedov, M.L. Rappaport, G. Jung, S. Bhattacharya, M.J. Higgins, Z.L. Xiao, E.Y. Andrei, P.L. Gammel, and D.J. Bishop, *Phys. Rev. Lett.* **85**, 3712 (2000).
35. B. Kalisky, A. Shaulov, T. Tamegai, and Y. Yeshurun, *Journal of Applied Physics* **93**, 8659 (2003).
36. Y.P. Sun, Y.Y. Hsu, B.N. Lin, H.M. Luo, and H.C. Ku, *Phys. Rev. B* **61**, 11301 (2000).
37. D. Giller, A. Shaulov, R. Prozorov, Y. Abulafia, Y. Wolfus, L. Burlachkov, Y. Yeshurun, E. Zeldov, V.M. Vinokur, J.L. Peng, and R.L. Greene, *Phys. Rev. Lett.* **79**, 2542 (1997).
38. M. Pissas, E. Moraitakis, G. Kallias, and A. Bondarenko, *Phys. Rev. B* **62**, 1446 (2000).
39. Y. Radzyner, S.B. Roy, D. Giller, Y. Wolfus, A. Shaulov, P. Chaddah, and Y. Yeshurun, *Phys. Rev. B* **61**, 14362 (2000).
40. T. Nishizaki, T. Naito, S. Okayasu, A. Iwase, and N. Kobayashi, *Phys. Rev. B* **61**, 3649 (2000).
41. N. Motohira, K. Kuwahara, T. Hasegawa, K. Kishio, and K. Kitazawa, *J. Ceramic Society of Japan* **97**, 1009 (1989).
42. M.C. de Andrade, N.R. Dilley, F. Ruess, and M.B. Maple, *Phys. Rev. B* **57**, R708 (1998).
43. M. Konczykowski, L.I. Burlachkov, Y. Yeshurun, and F. Holtzberg, *Phys. Rev. B* **43**, 13707 (1991).
44. L. Burlachkov, V.B. Geshkenbein, A.E. Koshelev, A.I. Larkin, and V.M. Vinokur, *Phys. Rev. B* **50**, 16770 (1994).
45. L. Burlachkov, *Phys. Rev. B* **47**, 8056 (1993).
46. L. Burlachkov, Y. Yeshurun, M. Konczykowski, and F. Holtzberg, *Phys. Rev. B* **45**, 8193 (1992).
47. E. Zeldov, D. Majer, M. Konczykowski, A.I. Larkin, V.M. Vinokur, V.B. Geshkenbein, N. Chikumoto, and H. Shtrikman, *Europhys. Lett.* **30**, 367 (1995).
48. V. Vinokur, B. Khaykovich, E. Zeldov, M. Konczykowski, R.A. Doyle, and P.H. Kes, *Phys. C* **295**, 209 (1998).
49. V.M. Vinokur, P.H. Kes, and A.E. Koshelev, *Phys. C* **168**, 29 (1990).
50. T. Giamarchi and P. LeDoussal, *Phys. Rev. B* **55**, 6577 (1997).
51. B. Kalisky, Y. Bruckental, A. Shaulov, and Y. Yeshurun, Submitted to *Phys. Rev. B*.